International Journal for Parasitology 49 (2019) 1049–1060

Contents lists available at ScienceDirect

International Journal for Parasitology

journal homepage: www.elsevier.com/locate/ijpara

Proteomic, metabolic and immunological changes in *Biomphalaria glabrata* infected with *Schistosoma mansoni*

Tiago Manuel Fernandes Mendes [a], Emanuel Carrilho [b,c], Ana Júlia Pinto Fonseca Sieuve Afonso [b,d], Carlos Alexandre Galinaro [b,c], Fernanda Janku Cabral [a], Silmara Marques Allegretti [a,*]

[a] Biology Institute, Animal Biology Department, Campinas State University (UNICAMP), SP, Brazil
[b] São Instituto de Química de São Carlos, Universidade de São Paulo, 13566-590 São Carlos, SP, Brazil
[c] Instituto de Ciência e Tecnologia de Bioanalítica – INCTBio, 13083-590 Campinas, SP, Brazil
[d] Medical Microbiology Unit, Global Health and Tropical Medicine (GHTM), Instituto de Higiene e Medicina Tropical (IHMT), Universidade Nova de Lisboa (UNL), Lisbon, Portugal

ARTICLE INFO

Article history:
Received 30 June 2019
Received in revised form 23 August 2019
Accepted 27 August 2019
Available online 11 November 2019

Keywords:
Biomphalaria glabrata
Immune response
Metabolism
Proteomics
Schistosoma mansoni

ABSTRACT

Mansonic schistosomiasis is a neglected disease transmitted by *Biomphalaria* spp. snails. Understanding what happens inside the intermediate host is important to develop more efficient ways of reducing schistosomiasis prevalence. Our purpose was to characterize metabolic and immunological changes in *Biomphalaria glabrata* 24 h after exposure to *Schistosoma mansoni*. For this purpose, proteins were extracted from snails' whole tissue with Tris-Urea buffer and digested with tripsin. Mass spectrometry was performed and analyzed with MaxQuant and Perseus software. Also, the hemolymph of five snails 24 h post exposure was collected, and the numbers of hemocytes, levels of urea, uric acid, nitric oxide, calcium, glycogen and alanine and aspartate aminotransferases activities were assessed. Snails were also dissected for measurement of glycogen content in the cephalopodal region and gonoda-digestive gland complex. Globin domain proteins were found to be up-regulated; also the number of circulating hemocytes was significantly higher after 24 h of exposure to the parasite. NO levels were higher 24 h post exposure. Several proteins associated with energy metabolism were found to be up-regulated. Glycogen analysis showed a significant decrease in the gonad-digestive gland complex glycogen content. We found several proteins which seem to be associated with the host immune response, most of which were up-regulated, however some were down-regulated, which may represent an important clue in understanding *B. glabrata* – *S. mansoni* compatibility.

1. Introduction

In Brazil, schistosomiasis is caused by *Schistosoma mansoni*, with *Biomphalaria glabrata* as its main intermediate host (Campos et al., 2002).

To detect the parasite and regulate the immune response against it, *B. glabrata* uses several toll-like receptors together with a signaling network for translational regulation through the nuclear transcription factor NF-kB (Adema et al., 2017). Other receptors include peptidoglycan recognition-binding proteins and gram-negative binding protein (Adema et al., 2017). After pathogen recognition, two main effector cell populations of hemocytes act in the snail immune defense system, granulocytes (with phagocytic activity) and hyalinocytes, as well as diverse soluble factors that are involved in pathogen recognition and inflammatory responses (Coustau et al., 2015; Giannelli et al., 2016).

Among described plasmatic proteins with immune potential against schistosome sporocysts, a major group belongs to the Variable Immunoglobulin and Lectin domain family (VIgL) (Wu et al., 2017). This family has three main categories, fibrinogen-related proteins (FREPs), galectin-related proteins (GREPs) and C-type lectin-related proteins (CREPs) (Dheilly et al., 2015; Adema et al., 2017; Wu et al., 2017).

FREPs is one of the most studied categories of VIgL, which suffers somatic mutations to generate unique FREPs repertoires in snails (Adema et al., 2017). FREPs have a highly conserved structure in several organisms, and it is the only known protein family in gastropods that combines immunoglobulin superfamily domains with fibrinogen domains (Giannelli et al., 2016). Among known FREPs subfamilies, some act as opsines for several mucines expressed in the surface of *Schistosoma* larvae (Giannelli et al., 2016; Galinier et al., 2017).

Another VIgL family that has been suggested to be implicated in the *B. glabrata* response to *S. mansoni* is GREPs. In work by Wu et al. (2017), GREP transcripts were found in 100% of infection-resistant

* Corresponding author.
E-mail address: sallegre@unicamp.br (S.M. Allegretti).

https://doi.org/10.1016/j.ijpara.2019.08.001
0020-7519/

snails. The same authors also found differential gene expression of this protein family, suggesting that different polymorphisms may be related to snail-parasite compatibility.

Besides VIgL, other proteins have been found to have important roles in the *B. glabrata* immune response against *S. mansoni*. *Biomphalaria* citolysine, biomphalysine, has shown high toxicity against the *S. mansoni* sporocyst, connecting to the parasite's membranes (Galinier et al., 2017; Mitta et al., 2017).

Adhesion hemocytes are highly phagocytic, producing reactive oxygen species (ROS) and nitric oxide (NO), important molecules for digenetic trematoda removal (Hahn et al., 2001a,b; Pereira et al., 2006). Previous studies have suggested that the specific allelic expression of Cu-Zn superoxide dismutase, enzymes responsible for H_2O_2 production (main ROS produced by *B. glabrata*), might be connected with the *B. glabrata* resistance phenotype against *S. mansoni* (Goodall et al., 2006; Bender et al., 2007). Another study has shown a correlation between high ROS production by snails and high anti-oxidative capability of their sympatric parasites. In said study, *S. mansoni* parasites from Brazil, with high anti-oxidative capability, were able to infect snails in allopatric combination, while the Guadalupe parasite (with lower anti-oxidative capability) was incompatible with Brazilian *B. glabrata* (Mone et al., 2011).

Heat-Shock proteins (HSPs) have also been studied in the snail-parasite context. Five families are known in *B. glabrata*, namely HSP20, HSP40, HSP60, HSP70 and HSP90. Among these, the HSP70 gene family is the largest with six genes containing several exons, five genes containing one exon and more than 10 pseudogenes (Adema et al., 2017). The connection of HSP70 with the *S. mansoni* sporocyst tegument was reported by Wu et al. (2017), however, although HSP70 expression increases during *Schistosoma* infection, in a study by Arican-Goktas et al. (2014), it was observed that an increase in HSP70 expression made the infection more permissive, and not only that, but the parasite could modulate the *B. glabrata* response through spatio-epigenetic control of gene expression. In the same study, resistant snails did not express HSP70 and stimulating HSP production made them more susceptible, while inhibiting HSP90 in susceptible snails reduced their susceptibility. Although the correlation between HSPs and *S. mansoni* is apparent, the functional connection (cause and effect) is yet to be established.

During parasitic infection, the host has higher energetic requirements, leading to an increase in carbohydrate mobilization and a decrease in hemolymph glucose content which is compensated by using energy reserves from either the digestive gland and/or cephalopodal region, and by increasing the activity of several energy-related metabolic pathways (Faro et al., 2013). Also, there is a higher calcium need, which not only plays an important role in the snail's immune system, but is also used as a cofactor in several metabolic pathways (Mostafa, 2007; Tunholi-Alves et al., 2014).

The obligatory need to infect and develop in an intermediate host during its life cycle, is the reason why it is important to understand what happens inside the snail during parasitic infection (Bayne, 2009). Immunological protein and gene regulation/expression studies are essential to understand the interactions between parasite and intermediate host (Giannelli et al., 2016). Therefore, it was our purpose to evaluate metabolic and immunological changes in *B. glabrata* after infection with *S. mansoni*.

2. Materials and methods

2.1. Parasites and animals

A *S. mansoni* BH (Belo Horizonte) strain kept in *B. glabrata* sympatric snails (~90% infection rate) at the Department of Animal Biology, Institute of Biology, Unicamp, Brazil, was used in this study. For life cycle maintenance, 30 days old Swiss female mice, weighting approximately 20 g each, obtained from the Multidisciplinary Centre for Biological Investigation (CEMIB), Unicamp, were individually infected with 70 cercariae by the tail immersion method (de Oliveira et al., 2017).

This study protocol (number 4024-1) was approved by the Ethics Commission for Animal Experimentation (CEEA) of the Biology Institute at Unicamp, as it was in accordance with the ethical principles adopted by the Brazilian Association of Animal Experimentation (COBEA).

2.2. Snail infection

Parasite eggs were collected from feces of infected mice, after filtration through 0.150 mm mesh. Hatching was stimulated in fresh water under incandescent light. Samples of miracidia were collected and counted. Eight miracidia were added per flask containing one snail each for 8 h under incandescent light. Snails used had approximately 8 mm shell diameters. The same procedure was performed for control snails (without exposure to miracidia).

2.3. Proteomic analysis

2.3.1. Protein extraction and digestion with trypsin

For proteomic analysis, three unexposed and three exposed (24 h post-exposure (pe)) snails were randomly selected. *Biomphalaria glabrata* whole tissue was homogenized (individually) in Tris-Urea buffer (50 mM Tris (Merck, Germany) pH 8.1, 75 mM NaCl (Merck), 8 M Urea (VWR, USA), protease and phosphatase inhibitor (VWR) and then centrifuged (Hettich® Universal 320R centrifuge, Andreas Hettich GmbH & Co. KG, Germany) at 20,000*g* for 15 min at 4 °C (Wu et al., 2014). The supernatant protein content was quantified using a Pierce BCA Protein Assay Kit (Thermo Scientific, Rockford, USA). Afterwards, 150 μg of protein were precipitated with acetone (Exodo Cientifica, Brazil) in the proportion 4:1 (v/v), incubated at −20 °C for 2 h and then centrifuged at 24,000*g* for 10 min at 4 °C. Precipitated proteins were then dissolved in 20 μL of 8 M urea (VWR), tested for pH (between 7 and 8), reduced with Dithiothreitol (DTT) (VWR) (5 mM final concentration) and incubated at 56 °C for 30 min. After reduction, samples were alkylated with iodoacetamide (IAA) (Sigma-Aldrich, USA) (14 mM final concentration) and incubated in the dark at room temperature for 15 min. Samples were then diluted 1:5 with 50 mM of NH_4HCO_3 (Sigma-Aldrich, USA) and then digested with trypsin (Promega, USA) in the proportion 1:50 (Enzyme: Substrate) and incubated at 37 °C for 16 h. Afterwards, samples were desalted using OASIS columns (Waters, Ireland), evaporated in a speedvac (Vacufuge®Plus, Eppendorf, Germany) and kept at −20 °C until LC-MS/MS analysis.

2.3.2. LC-MS/MS analysis

Processed peptides were solubilized in 12 μL of 0.1% formic acid and 4 μL were analyzed in an Easy-nLC II nanoflow liquid chromatograph system (Thermo Fisher Scientific, Waltham, MA, USA) in tandem with a LTQ-Orbitrap Velos mass spectrometer (Thermo Fisher Scientific), which was equipped with a nanoelectrospray Nano-Flex II (Thermo Fisher Scientific) operating in positive ion mode. Nanoeletrospray voltage was set to 2.3 kV and source temperature at 250 °C. The precursor ion was isolated using the data-dependent acquisition mode with a 2 m/z isolation width, and sequentially, the 10 most intense ions were selected for the fragmentation event by collision induced dissociation (CID), at 35% normalized collision energy and 10 ms activation time. Maximum ion injection times were set to 100 ms for MS and 500 ms for MS/MS, with a resolution of 60,000 and a scan within m/z range from 300 to 1800. Chromatographic separation was carried out a Thermo

C18 capillary column (10 cm × 75 μm, 3 μm, 120 Å) protected by a guard Thermo C18 capillary column (2 cm × 100 μm i.d., 5 μm particle, 120 Å pore size). Water containing 0.1% formic acid (Sigma-Aldrich/Merck, Darmstadt, Germany) (solvent A) and acetonitrile MS grade (Sigma-Aldrich/Merck) containing 0.1% formic acid (solvent B) were used as a mobile phase. The separation was performed at room temperature with a constant flow rate of 0.2 μL/min, with a total acquisition time of 145 min, by employing the elution program as follows: 5% solvent B increasing to 40% of solvent B in 90 min, to 99% solvent B at 20 min, followed by isocratic elution with solvent B for 20 min, to 136 min at 5% solvent B and 5% solvent B held for 9 min. Data acquisition was controlled by Xcalibur 2.0.7 Software (Thermo Fisher Scientific, Waltham, MA, USA).

2.3.3. Proteomic analysis

MS/MS spectra (raw data) were processed with MaxQuant using the LFQ (Label Free Quantification) (Cox and Mann, 2008) for quantification of more intense precursor ions. Protein searches were performed using *fasta* files from three *B. glabrata* databases (NCBI, ncbi.nlm.nih.gov; Uniprot, www.uniprot.org; vectorbase, www.vectorbase.org) (information from the databanks used was downloaded on October 10, 2017). For peptide identification confidence, mass tolerance for precursor ions was set at 4.5 ppm and 20 ppm for ion fragments. Methionine oxidation and N-acetylation were chosen as fixed modifications and carbamidomethyl as a variable modification. Identification was considered for peptides that presented as having more than three unique peptides identified. The resulting protein group list was analyzed using Perseus software version 1.5.2.6 (Tyanova et al., 2016). Firstly, contaminants were filtered (valid for at least three samples of one group), and an experimental quality check was carried out using Perseus tools such as multi-scatter plots and hierarchical clustering (Supplementary Figs. S1 and S2). Proteins were considered down- or up-regulated when $P < 0.05$, Student's *t* test. To analyze Gene Ontology (GO) components, differentially expressed proteins (molecular functions, cellular components and biological processes) were searched using protein domains/-families available on vectorbase.

2.4. Hemolymph analysis

For hemolymph analysis, five unexposed and five exposed (24 h pe) snails were randomly selected. Hemolymph was collected and analyzed individually.

2.4.1. Hemocyte count

Hemocytes were counted using a Neubauer chamber. Hemolymph was diluted (1/10) in Chernin Balanced Salt Solution (CBSS – 48 mM NaCl, 2.0 mM KCl (Merck), 0.5 mM Na_2HPO_4 (Merck), 1.8 mM $MgSO_4{\cdot}7H_2O$ (Merck), 3.6 mM $CaCl_2{\cdot}2H_2O$ (Sigma-Aldrich), 0.6 mM $NaHCO_3$ (Merck), 5.5 mM glucose (Merck) and 3 mM threalose (Inlab, Brazil), pH 7.4) containing 0.05% Neutral Red (Sigma-Aldrich) and counted in a Neubauer chamber under a microscope (Leica DM500, Leica, Germany). Stained cells were considered granulocytes (Martins-Souza et al., 2003).

2.4.2. NO

NO was indirectly estimated through measurement of nitrite levels using a Griess reaction. Briefly, a solution containing 10 μL of whole hemolymph, 100 μL of Griess reagent (Sigma-Aldrich) and 100 μL of 10% trichloroacetic acid (Exodo Cientifica) was incubated for 10 min at room temperature and centrifuged at 3000*g* for 5 min. The supernatant (200 μL) was transferred to a 96 well plate and absorbance was measured at 600 nm (AgileReader AMPR-900, Avans Biotechnology, Taiwan). The amount of NO was estimated from a standard curve of $NaNO_2$ (Sigma-Aldrich) (Pereira et al., 2006).

2.4.3. Urea

The urea concentration was measured mixing 1 μL of whole hemolymph with 100 μL of urease buffer (19.1 mM phosphate buffer, 59.3 mM sodium salicylate, 3.2 mM sodium nitroprusside and 13.4 kU/L of urease; Labtest, Brazil). The mixture was incubated at 37 °C for 5 min. After incubation, 100 μL of oxidant solution (2.7 M sodium hydroxide, 115 mM sodium hypochlorite; Labtest) were added and incubated for another 5 min at 37 °C. Measurements were made at 600 nm (AgileReader AMPR-900). The concentration was estimated from a standard curve of urea and expressed in μg/μL (Searcy et al., 1967).

2.4.4. Aminotransferase activity

Aminotransferase activity was measured according to Tunholi-Alves et al. (2012). Briefly, 16.1 μL of substrate for ALT or AST (solution containing 0.2 M L-alanine or 0.2 M L-aspartate(Dinamica, Brazil), respectively, 0.002 M α-ketoglutarate (Sigma-Aldrich) and 0.1 M sodium phosphate buffer, pH 7.4) was incubated for 2 min at 37 °C for 2 min, and then mixed with 6.5 μL of whole hemolymph. The mixture was homogenized and incubated for 30 min at 37 °C. After incubation, 16.1 μL of 0.001 M 2,4-dinitrophenylhydrazine (Sigma-Aldrich) were added and kept at 25 °C for 20 min. The reaction was stopped by adding 161.3 μL of 0.4 M NaOH (Sigma-Aldrich). Readings were made in a spectrophotometer (AgileReader AMPR-900) at 490 nm and the results expressed as U/mL.

2.4.5. Glycogen concentration

To determine glycogen concentration, whole hemolymph (13 μL) was mixed with 33 μL of phenol 5% (Sigma-Aldrich), then 133 μL of H_2SO_4 96–98% (Exodo Cientifica) were added and the mixture was incubated at room temperature for 10 min, followed by another incubation at 30 °C for 20 min. Readings were performed at 490 nm (AgileReader AMPR-900), and the concentration was estimated from a standard curve of glycogen (Sigma-Aldrich) and expressed in μg/μL (Lo et al., 1970).

2.4.6. Calcium concentration

The calcium concentration of snail hemolymph was measured based on the principle that O-cresolphthalein complexone reacts with calcium in alkaline solution to form a purple colored complex (Chilcote and Wasson, 1958). Briefly, whole hemolymph (4 μL) was added to each well of a 96 well plate, then 196 μL of a solution (Laborclin, Brazil) containing 0.08 mM O-cresolphthalein complexone and 4.5 mM 8-hydroxyquinoline were added and homogenized. Plates were incubated at room temperature for 1 min and measured at 600 nm (AgileReader AMPR-900). The calcium concentration was estimated from a standard curve of $CaCO_3$ (Sigma-Aldrich) and expressed in μg/μL.

2.5. Glycogen tissue content

The cephalopodal region and gonad-digestive gland complex were dissected from five unexposed and five exposed (24 h pe) snails. Glycogen extraction was performed individually according to Pinheiro et al. (2001). Briefly, tissues were weighed and homogenized in 10% trichloroacetic acid (Exodo Cientifica) (10 mL per g of tissue) and centrifuged at 2000*g* for 20 min at 4 °C. Supernatant was filtered in Whatman paper n° 1. Iced ethanol (2:1) was mixed with the filtered supernatant and incubated on ice for 15 min followed by centrifugation at 2000*g* for 10 min at 4 °C. The supernatant was discarded and the pellet was resuspended in 1 mL of H_2O. An aliquot of 1 mL of 1 M HCl (Labsynth, Brazil) was added for glycogen hydroxylation and incubated for 30 min at 100 °C. Glycogen was

then stored at −20 °C until analyzed. For quantification, extracted glycogen pH was neutralized using 1 M NaOH (Sigma-Aldrich). The glycogen concentration was determined using 33 μL of extracted glycogen, mixed with 33 μL of phenol 5% (Sigma-Aldrich). Then 133 μL of H_2SO_4 96–98% (Exodo Cientifica) were added and incubated at room temperature for 10 min, followed by another incubation at 30 °C for 20 min. Readings were performed twice per sample at 490 nm (AgileReader AMPR-900), and the concentration was estimated from a standard curve of glycogen and expressed in μg of glycogen/mg of wet tissue (wt) (Lo et al., 1970).

2.6. Statistical analysis

Statistical tests were performed with GraphPad Prism 7 software. Student's *t* test was used to analyze significant differences between groups, where $P < 0.05$ was considered significant.

3. Results

3.1. Proteomic analysis

Using MaxQuant (Cox and Mann, 2008; Tyanova et al., 2016) and Perseus software, a combined total of 2213 proteins was identified out of which 402 were valid for at least three samples of one group. Out of 402 proteins, 29 were considered to be up-regulated (Table 1) and 10 down-regulated (Table 2) ($P < 0.05$, Student's *t* test) in snails exposed to *S. mansoni* (Supplementary Fig. S3, Supplementary Data S1).

3.2. GO of differently expressed proteins

Protein sequences (Supplementary Tables S1 and S2) were searched in Blastp (NCBI) for protein identification and in vectorbase for domains and respective GO identification (Supplementary Tables S3 and S4). The most common biological process (GO) in up-regulated proteins was oxidation–reduction process (GO:00055114), followed by proteolysis (GO:0006508) (Fig. 1). With regard to molecular function (GO), among the up-regulated proteins the most common was heme binding (GO:0020037), followed by catalytic activity (GO:0003824), whilst in down-regulated proteins the most common molecular function was protein binding (GO:0005515) (Fig. 2). The cellular component (GO) most commonly found in up-regulated proteins was the nucleosome (GO:0000786) and in down-regulated proteins was the extracellular region (GO:0005576) (Fig. 3).

3.3. Hemolymph analysis

The number of circulating hemocytes was significantly higher 24 h pe ($P < 0.05$). The number of circulating granulocytes did

Table 1
Up-regulated proteins found in *Biomphalaria glabrata* 24 h after exposure to *Schistosoma mansoni*.

Protein ID	Protein name	Peptides	Unique peptides	Sequence coverage (%)	MW (kDa)	Score	Intensity	MS/MS count
XP_013088291.1[a]	collagen alpha-5(VI) chain-like	13	13	43.2	42.571	59.904	6.91E + 08	26
CAJ44467.1[a]	haemoglobin type 2	108	13	69.6	196.750	323.310	3.47E + 10	730
BGLB029153-PA[b]	transgelin-3-like	12	12	63.6	18.307	141.650	2.04E + 09	60
XP_013072912.1[a]	uncharacterized protein LOC106059779	4	4	24.0	51.342	227.960	6.36E + 08	19
BGLB004011-PB[b]	phosphoglycerate mutase	9	9	55.8	28.590	37.668	3.31E + 08	29
XP_013082420.1[a]	14-3-3 protein epsilon-like	9	9	38.0	29.234	140.920	1.35E + 09	58
XP_013080331.1[a]	4-hydroxyphenylpyruvate dioxygenase-like	10	10	39.8	43.516	54.488	1.05E + 08	23
XP_013083901.1[a]	actin, cytoplasmic-like	32	7	77.0	59.597	181.290	1.05E + 10	134
tr|D8V7I9|D8V7I9_BIOGL[c]	arginine kinase	37	20	91.2	39.297	323.310	1.16E + 10	248
tr|A0A182Z3P7|A0A182Z3P7_BIOGL[c]	ATP synthase subunit beta, mitochondrial-like	19	17	54.3	56.762	225.660	2.36E + 09	89
tr|A0A182YYT2|A0A182YYT2_BIOGL[c]	core histone H2A/H2B/H3/H4	3	3	18.5	14.018	18.433	4.44E + 08	10
XP_013066286.1[a]	endoglucanase A-like	7	7	23.1	50.732	25.797	1.85E + 08	13
tr|A0A182YWZ1|A0A182YWZ1_BIOGL[c]	endoglucanase E-4-like	17	11	40.0	95.921	299.420	1.65E + 09	74
XP_013089012.1[a]	gelsolin-like protein 2	5	5	25.1	39.034	43.428	1.12E + 08	13
BGLB018373-PA[b]	globin-like	8	3	58.5	13.461	71.852	7.38E + 08	32
XP_013093671.1[a]	glucose dehydrogenase [FAD, quinone]-like	11	11	31.0	53.425	35.382	3.95E + 08	23
tr|A0A182ZSX0|A0A182ZSX0_BIOGL[c]	guanine nucleotide-binding protein subunit beta	7	7	34.6	37.252	69.092	1.68E + 08	14
tr|A0A182ZWC2|A0A182ZWC2_BIOGL[c]	haemoglobin type 2	99	13	72.5	158.370	323.310	1.69E + 09	68
tr|Q14SM7|Q14SM7_BIOGL[c]	haemoglobin type 2	116	16	72.8	196.75	323.310	3.53E + 10	787
XP_013078918.1[a]	histone H3-like	3	3	20.2	11.342	37.148	4.44E + 08	13
BGLB019194-PA[b]	uncharacterized protein LOC106051722	35	28	42.7	88.413	323.310	1.39E + 10	221
BGLB011523-PB[b]	uncharacterized protein LOC106077292	13	6	7.9	223.45	39.774	1.31E + 09	34
tr|A0A182ZCF8|A0A182ZCF8_BIOGL[c]	mitochondrial-processing peptidase subunit beta-like	6	6	25.9	44.458	48.618	1.67E + 08	14
tr|A0A182YUV3|A0A182YUV3_BIOGL[c]	myophilin-like	5	5	36.4	22.990	41.675	2.24E + 08	14
XP_013081220.1[a]	myosin essential light chain, striated adductor muscle-like	7	7	67.7	18.228	35.015	4.58E + 08	21
XP_013079848.1[a]	transforming growth factor-beta-induced protein ig-h3-like	7	7	17.2	68.859	93.954	5.37E + 08	18
BGLB012730-PB[b]	uncharacterized protein LOC106050211	22	10	50.3	61.458	100.350	3.22E + 09	91
XP_013062423.1[a]	uncharacterized protein LOC106051763	94	13	55.9	192.120	126.950	8.91E + 08	31
BGLB018374-PA[b]	uncharacterized protein LOC106051916	87	69	71.5	139.080	323.310	3.27E + 10	661

[a] NCBI database ID.
[b] Vectorbase database ID.
[c] Uniprot database ID.

Table 2
Down-regulated proteins found in *Biomphalaria glabrata* 24 h after exposure to *Schistosoma mansoni.*

Protein ID	Protein name	Peptides	Unique peptides	Sequence coverage (%)	MW (kDa)	Score	Intensity	MS/MS count
BGLB017153-PE[a]	filamin-A-like isoform X4	55	55	36.7	256.870	323.310	2.86E + 09	199
BGLB000137-PB[a]	biomphalysin	13	2	28.7	64.808	74.982	2.66E + 08	5
XP_013073862.1[b]	retrograde protein of 51 kDa isoform X2	53	53	80.2	65.281	323.310	6.44E + 09	287
tr|A0A182Z4N2| A0A182Z4N2_BIOGL[c]	mammalian ependymin-related protein 1-like	9	9	34.6	27.251	138.890	1.32E + 09	71
BGLB004497-PB[a]	elongation factor 1-gamma-like	7	7	17.5	49.142	22.927	59,085,000	22
XP_013065737.1[b]	troponin I-like isoform X10	22	3	45.3	41.564	220.780	1.,15E + 09	94
BGLB009133-PB[a]	SCO-spondin-like	4	4	3.6	236.730	49.259	40,341,000	10
tr|A0A182ZAQ2| A0A182ZAQ2_BIOGL[c]	cathepsin L1-like	4	3	25.8	19.640	46.394	1.24E + 08	14
BGLB023192-PA[a]	endo-1,4-beta-xylanase A-like	9	9	19.6	87.938	52.857	1.5E + 08	20
BGLB016564-PA[a]	sarcoplasmic/endoplasmic reticulum calcium ATPase 1-like	15	15	27.6	108.660	76.358	3.6E + 08	27

[a] Vectorbase database ID.
[b] NCBI database ID.
[c] Uniprot database ID.

not differ significantly after exposure (Fig. 4A, B). NO (Fig. 4C) and urea (Fig. 4D) levels, ALT and AST activities (Fig. 4E, F) were significantly higher ($P < 0.05$) in exposed snails. We did not find a significant difference in hemolymph glycogen content (Fig. 4G). Hemolymph calcium concentration (Fig. 4H) was significantly lower ($P < 0.05$) in snails 24 h pe.

3.4. Glycogen tissue content

Glycogen content was significantly higher ($P < 0.05$) in the cephalopodal region 24 h pe (Fig. 5A). In the gonad-digestive gland complex, the glycogen concentration was significantly lower 24 h pe ($P < 0.05$) (Fig. 5B).

4. Discussion

Hemocytes, particularly granulocytes, are the main immune cells in *B. glabrata*. Our results showed a significantly higher number of hemocytes in the snail hemolymph (Fig. 6A), however there was no significant difference in the number of granulocytes (Fig. 6B). According to Pereira et al. (2006), during infection the number of circulating hemocytes does not always increase, likely due to migration towards the place of infection (Fig. 6B1), which might explain why we did not find a significant increase in granulocytes. Also, similar to Wu et al. (2017), the most commonly found proteins were Globin Domain proteins (hemoglobin type 2 and globin-like proteins) (Fig. 6C). Another work by Tetreau et al. (2017) reported that, while hemoglobin-1 and -2 were identified against *Escherichia coli,* only hemoglobin-2 was found interacting with *Echinostoma caproni* and *S. mansoni*, suggesting that hemoglobin-2 might be more specific to trematode infections.

Several of the proteins found up-regulated in exposed snails are involved in energy production. Endoglucanase A-like and endoglucanase E-4-like are both cellulases, breaking down cellulose into monosaccharides such as β-glucose (Fig. 7E). 4-Hydroxyphenylpyruvate dioxygenase-like is involved in breaking L-tyrosine into acetoacetate and fumarate, indicating activation of the tricarboxylic acid (TCA) cycle (Silva et al., 2017) (Fig. 7F). Arginine kinase belongs to the phosphagen kinase family and has a significant role in maintaining energy homeostasis, catalyzing the reversible transfer between phosphagens and ATP (Jarilla et al., 2014). Glucose dehydrogenase [FAD, quinone]-like is an oxidoreductase that participates in the pentose phosphate pathway (Fig. 7G) and phosphoglycerate mutase is an enzyme that catalyzes the 8th step in glycolysis (Fig. 7H), with both enzymes contributing to ATP production. ATP synthase subunit beta, a mitochondrial protein, is also involved in the production of ATP from ADP (Fig. 7I). Up-regulation of all these proteins in exposed *B. glabrata* suggests that there is an attempt by the mollusk to compensate for increased energetic requirements, leading to an increase in ATP production (Fig. 7J).

Previous work by Lewert and Para (1966), using 14C-glucose, has shown that *S. mansoni* has a remarkable ability to absorb the host's glucose, as early as 24 h after exposing the snail to radioactive medium. Cheng and Lee (1971) have also shown that hemolymph glucose levels in *S. mansoni*-exposed snails lowers significantly compared with unexposed snails, presumably, in part, due to parasite absorption. Similar to Lewert and Para (1966), Christie et al. (1974) also used 14C-glucose to study *S. mansoni* glucose consumption; the authors reported that developing parasites use at least 12.6% of the initial label absorbed by the snail and, furthermore, glycogen depletion occurs more quickly in infected *B. glabrata* compared with starved snails, suggesting that the rapidly developing parasite is actively using the host's glycogen stores. The authors also found that the label presence in the albumen gland was much lower in infected snails. Similar to the authors, we found that there was a significant decrease in glycogen in the gonad-digestive gland complex (Fig. 7A). Interestingly however, we found an increase in the glycogen content of the cephalopodal region (Fig. 7B), which likely happens due to a mobilization of glycogen reserves (from the gonad-digestive gland complex) to this region where there is an increased energetic need due to the presence of the sporocyst. We did not find changes in hemolymph glycogen content (Fig. 7C), suggesting there is also a mobilization towards the hemolymph to promote glucose homeostasis (Faro et al., 2013). Furthermore, it has been suggested that, to compensate for the decrease in glycogen content, there is an increase in gluconeogenesis (Mello-Silva et al., 2010). Our results also seem to agree, since we found an increase for both AST and ALT activities and these aminotransferases are enzymes that play an important role in gluconeogenesis and in TCA (Fig. 7D), deaminating amino acids that are transferred to these pathways (Pinheiro et al., 2001). Protein and amino acid deamination, as well as the increase in NO, leads to an accumulation of nitrogen products which are toxic to the snail. To deal with this accumulation, there is an increase in the urea pathway, and the snail stops being ammoniotelic, instead becoming ureotelic, resulting in the observed increase in urea (Becker and Schmale, 1975; Souza et al., 2000).

Calcium is an important mineral involved in redox reactions as an enzyme cofactor, is involved in metabolic processes related to acid-base balance and plays an important role in the snail's

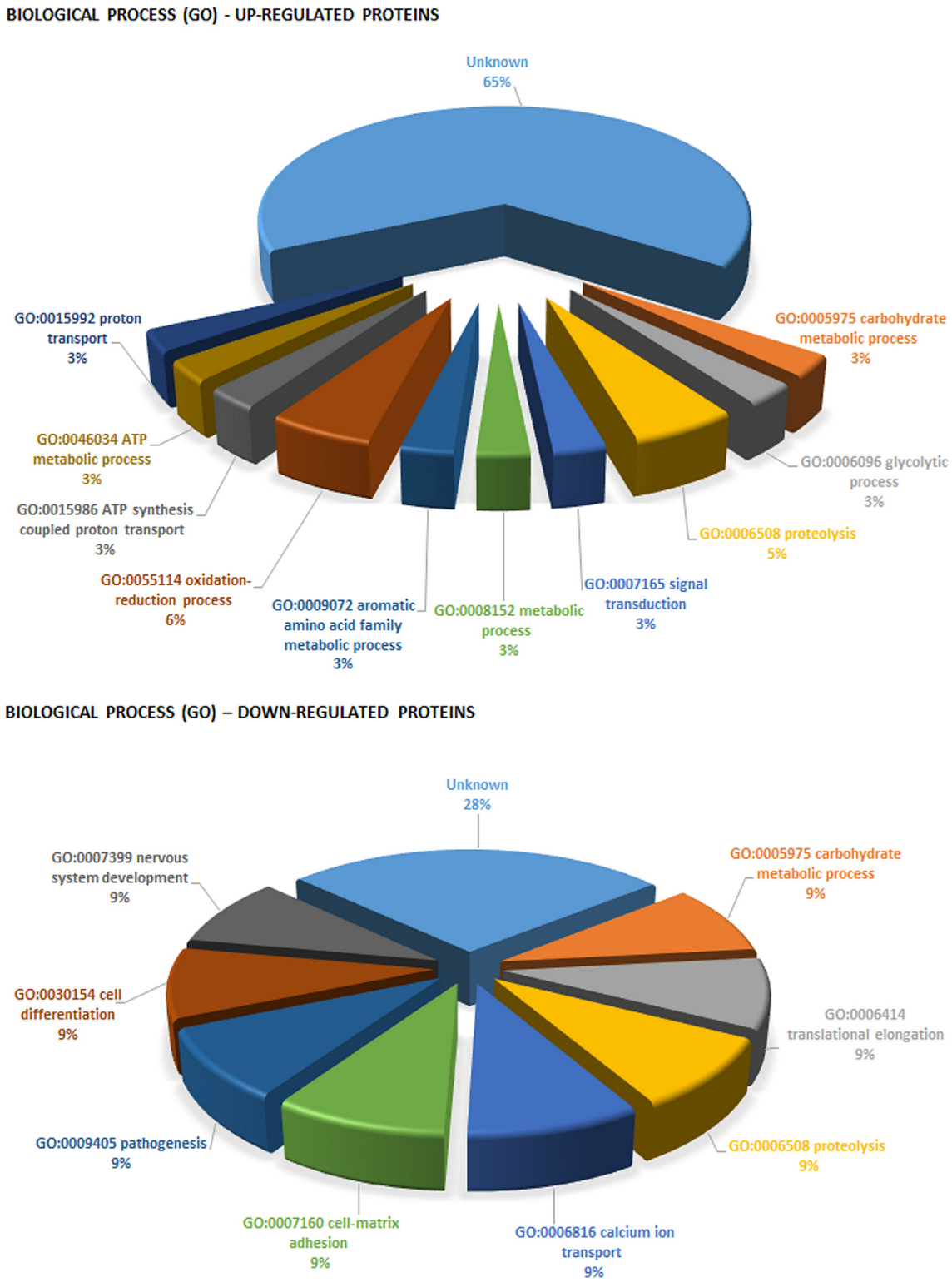

Fig. 1. Biological process Gene Ontology of differentially expressed proteins found in *Biomphalaria glabrata* 24 h post exposure to *Schistosoma mansoni*.

immune response (Sminia et al., 1977; de Witt and Sminia, 1980; Tunholi-Alves et al., 2014). Calcium is also used by parasites to maintain their life cycle inside the intermediate host. Shaw and Erasmus (1987) found a significant depletion in *B. glabrata* calcium reserves just 48 h after *S. mansoni* infection, whilst Tunholi-Alves et al. (2014) found a decrease in hemolymph calcium content in the first and second weeks after *Angiostrongylus cantonensis* infection. Therefore, the decrease in calcium in the exposed snails' hemolymph (Fig. 6D) may be attributed to the higher need of this ion, not only by the parasite that absorbs calcium for its development and metabolic requirements (Fig. 6D2), but also due to the increased energetic needs of the mollusk, which are obtained mainly through oxidative reaction catalyzed by enzymes that use calcium as a cofactor (Tunholi-Alves et al., 2014) (Fig. 6D3).

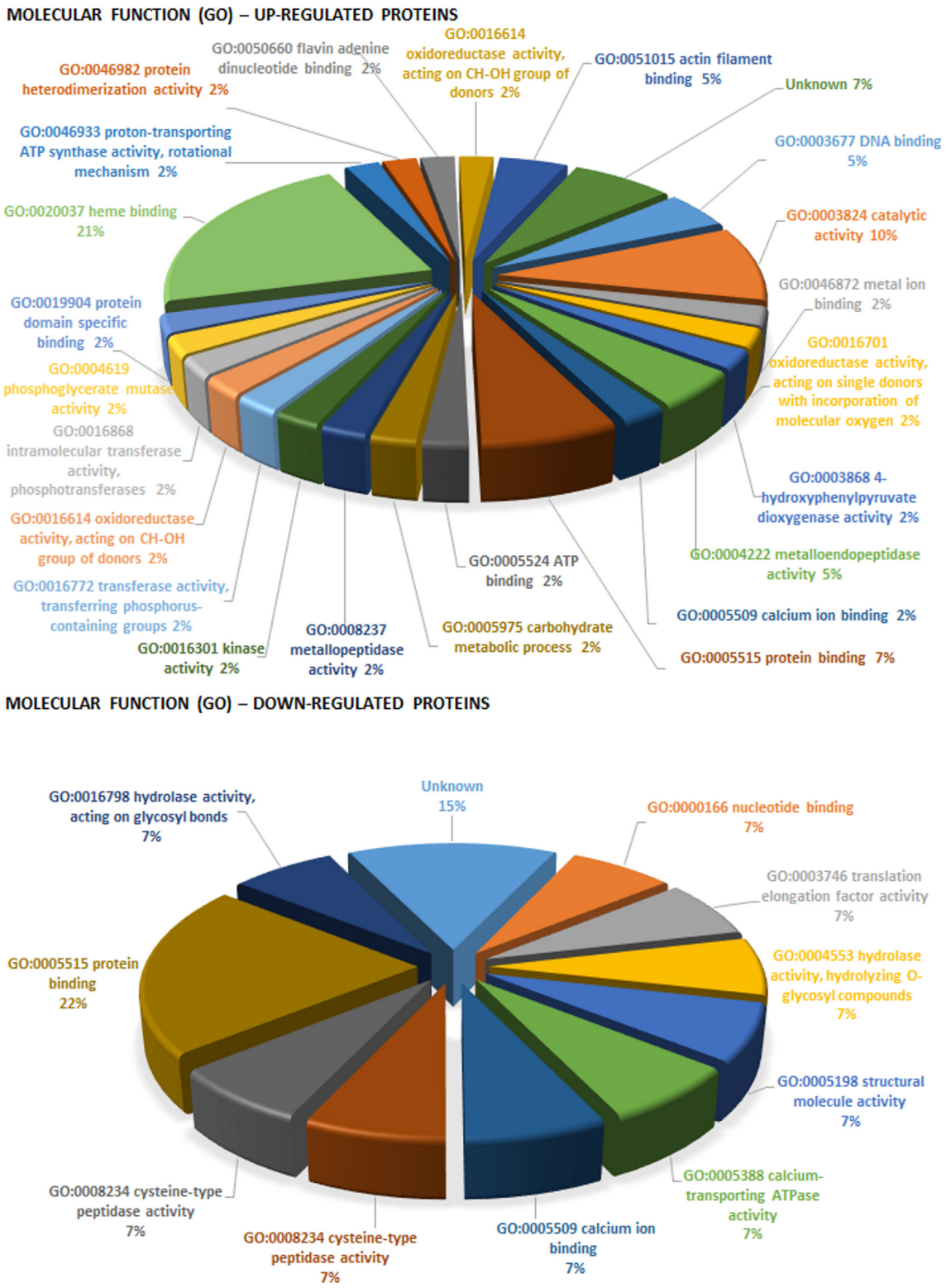

Fig. 2. Molecular function Gene Ontology of differentially expressed proteins found in *Biomphalaria glabrata* 24 post exposure to *Schistosoma mansoni*.

Furthermore, the damage caused by the parasite in the tissues may cause a decrease in hemolymph calcium levels, since this ion is deposited in the host tissues in response to inflammatory reactions caused by the parasite (Fig. 6D1) (Mostafa, 2007; Tunholi-Alves et al., 2014).

Cytoplasmic-like actin was found to be up-regulated in exposed snails (Fig. 6E). In the mosquito Anopheles gambiae, cytoplasmic actin is an important extracellular immune factor that mediates phagocytosis (Sandiford et al., 2015), whilst in *B. glabrata* it has been shown that cytoplasmatic actin is capable of binding and participates in clotting of yeast cells prior to its elimination (Tetreau et al., 2017). Therefore it is possible that a similar phenomenon occurs in snails, where actin connects to the sporocyst marking it for phagocytosis (Fig. 6E1). It is interesting to notice, however, that

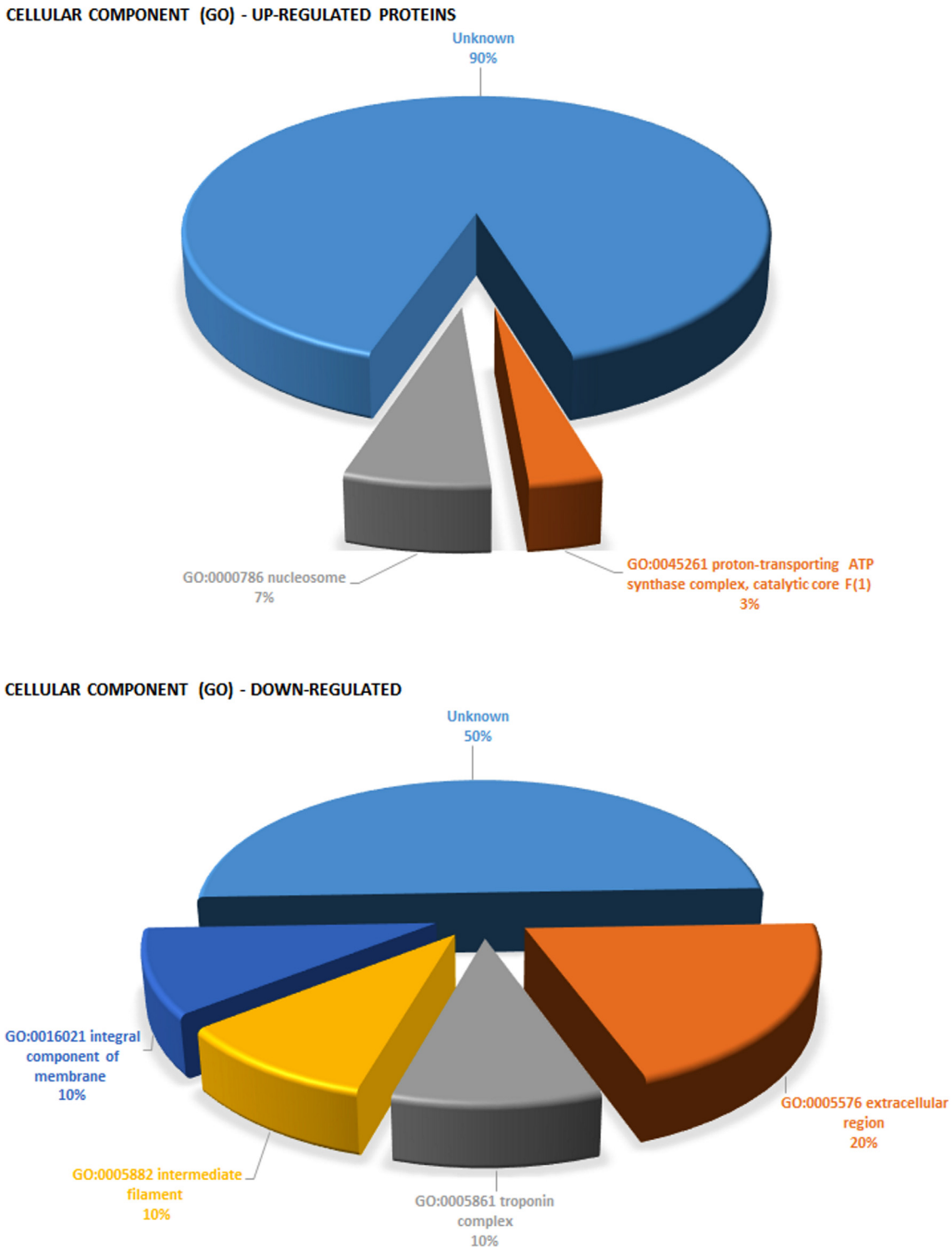

Fig. 3. Cellular component Gene Ontology of differentially expressed proteins found in *Biomphalaria glabrata* 24 post exposure to *Schistosoma mansoni*.

Arican-Goktas et al. (2014) have shown that in BS-90 snails (*S. mansoni*-resistant snails) there was a 22 fold increase in actin expression 30 min after parasite exposure, with no major gene loci repositioning, while in NMRI snails (*S. mansoni*-susceptible snails), actin gene loci took 1.5 h for repositioning and 2 h to increase expression by 16 fold, suggesting that not only the increase in actin is important, but also how fast this increase occurs.

Gelsolin-like protein 2 is an actin-binding protein, which we found to be up-regulated in exposed *B. glabrata* (Fig. 6F). Gelsolins are key regulators of actin filament assembly and disassembly. Previous reports have shown that in plants, as a response to microbial signals, gelsolins play an important role, exposing actin filaments for C-type lectin receptors (Sandiford et al., 2015). Overexpression of this protein in mollusks may have a similar role in exposing the sporocyst actin filaments to *B. glabrata*'s C-type lectin-related proteins (Fig. 6F1).

Adema et al. (2010) found up-regulated sequences encoding histones H2A, H2AV and H3.3, of which histone H3.3 had the highest

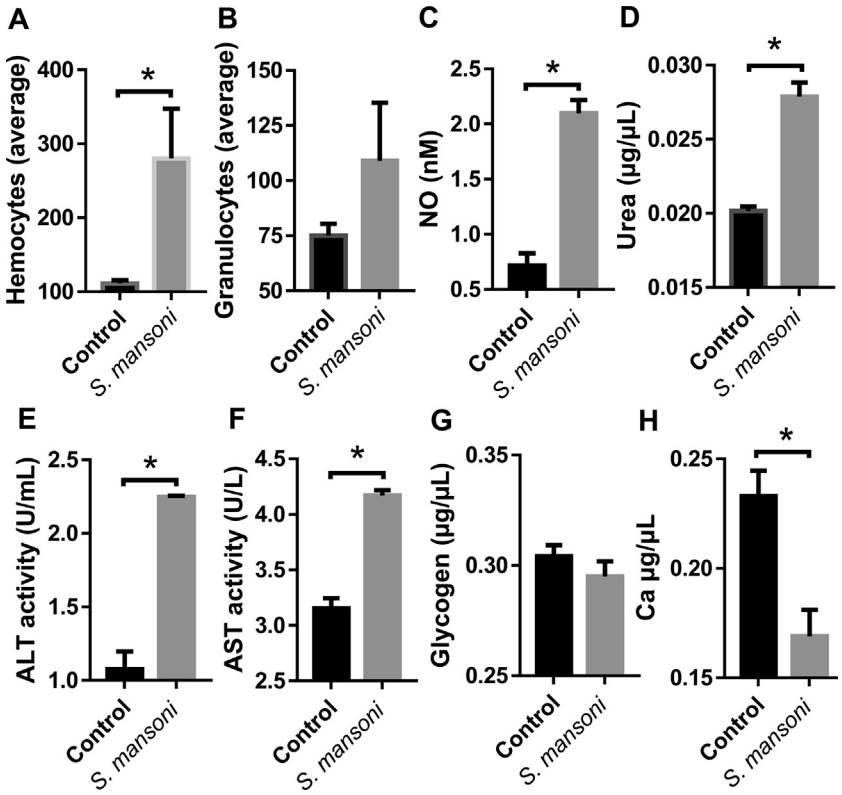

Fig. 4. Hemolymph analysis of *Biomphalaria glabrata* snails 24 h post exposure to *Schistosoma mansoni* and the respective uninfected control group. (A) Average number of hemocytes; (B) average number of granulocytes; (C) hemolymph nitric oxide content; (D) hemolymph urea content; (E) alanine-aminotransferase activity; (F) aspartate-aminotransferase activity; (G) hemolymph glycogen content; (H) hemolymph calcium content. * Significant difference between control and infected snails (Student's *t* test, $P < 0.05$).

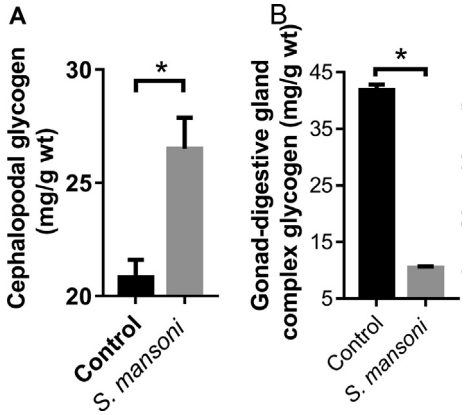

Fig. 5. Tissue analysis of *Biomphalaria glabrata* snails 24 h post exposure to *Schistosoma mansoni* and the respective uninfected control group. (A) Cephalopodal glycogen content; (B) gonad-digestive gland complex glycogen content. * Significant difference between control and infected snails (Student's *t* test, $P < 0.05$). wt – wet tissue.

expression. Similarly, we found core histone H2A/H2B/H3/H4 and histone H3-like were up-regulated. Histones play a role in chromatin remodeling during mitosis, act as receptors for viruses and bacteria at the cell surface, are components of extracellular traps, and exert direct bactericidal activity (Sandiford et al., 2015), therefore their up-regulation in exposed snails is not surprising.

Guanine nucleotide-binding proteins (G-proteins) are proteins involved in several signal transduction pathways (Spiegel, 1987), while transforming growth factor-beta-induced protein ig-h3-like (TGF-β) and 14-3-3 protein epsilon-like are signaling proteins. Similar to our results, Zhang et al. (2015) found G-proteins over-expressed in *B. glabrata* after exposure to molluscicide, while Wu et al. (2017) found TGF-β and 14-3-3 proteins over-expressed in snails exposed to *S. mansoni*, which might indicate that these proteins could be involved in the snail's response to stress (Fig. 6G).

The uncharacterized protein LOC106059779 is a protein with a Peptidase M12B, ADAM/reprolysin domain that was over-expressed in exposed snails. Proteins with this domain are matrix metalloproteinases that function in tissue morphogenesis/remodeling and inflammation, and have been associated with larval binding activity. Wu et al. (2017) also found ADAM-TS proteins were differentially expressed at both the plasma protein and transcript levels in susceptible NMRI snails. According to the authors, a relatively high level of circulating ADAM-TS may be advantageous to the parasite by degrading endogenous host matrix proteins, facilitating larval movement through snail tissues.

In the *B. glabrata* immune system, hemocytes produce ROS and NO to fight the infection (Hahn et al., 2001a,b; Pereira et al., 2006), therefore is not surprising that NO levels were significantly higher in exposed snails. Filamin A (FlnA) is known to be an important actin cross-linking protein required for cellular processes such as cell migration. This protein role in *B. glabrata* is not well defined, however, in a transgenic mouse model, FlnA has been shown to be a negative regulator of β2 integrin-dependent cell adhesion and ROS production (Uotila et al., 2017). Exposed snails shown down-regulation of this protein (Fig. 6H), suggesting that possibly, in *B. glabrata*, hemocyte adhesion and ROS production are also negatively regulated by FlnA.

Mammalian ependymin-related protein 1-like is an adhesion molecule that displays similarities to mammalian ependymin related proteins (MERPs). These proteins are extracellular matrix constituents with anti-adhesive properties (Bouchut et al., 2007).

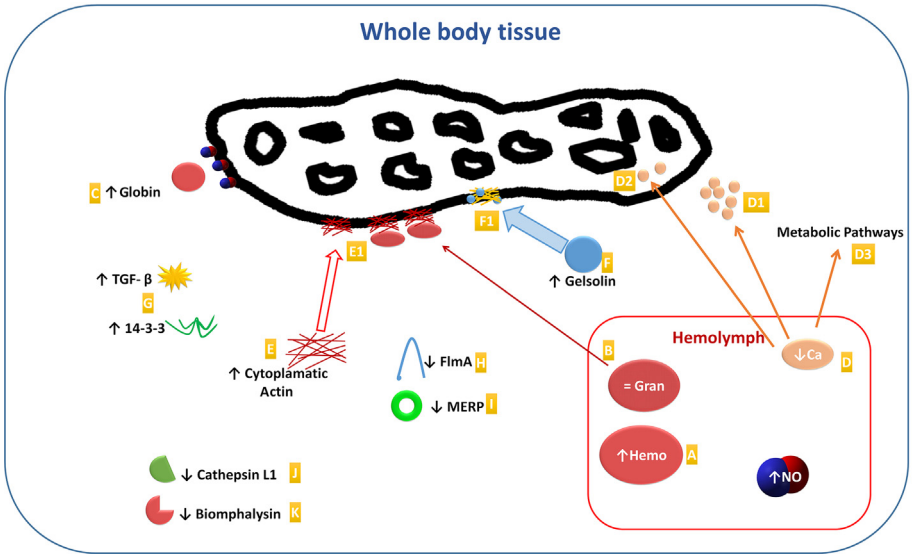

Fig. 6. Immune response related changes in *Biomphalaria glabrata* 24 h post exposure to *Schistosoma mansoni*. (A) Significant increase in the number of hemocytes. (B) No significant difference in the number of granulocytes in the hemolymph, most likely due to migration towards the place of infection in the tissue. (C) Up-regulation of hemoglobin type 2 and globin-like proteins. (D) Decrease in hemolymph calcium content due to (D1) deposit in the host tissues as a response to inflammatory reactions, (D2) parasite absorption and (D3) use in several metabolic pathways. (E) Up-regulation of cytoplasmic-like actin; (E1) connecting with the sporocyst, marking it for phagocytosis. (F) Up-regulation of Gelsolin-like protein 2, exposing the sporocyst actin filaments. (G) Up-regulation of signaling proteins transforming growth factor-beta-induced protein ig-h3-like (TGF-β) and 14-3-3 protein epsilon-like. (H) Down-regulation of Filamin A, a negative regulator of cell adhesion and of reactive oxigen species production. (I) Down-regulation of mammalian ependymin-related protein 1-like, a protein with anti-adhesive properties that would interfere with parasite encapsulation. (J) Down-regulation of biomphalysin. (K) Down-regulation of Cathepsin L1-like, a protein involved in phagocytosis.

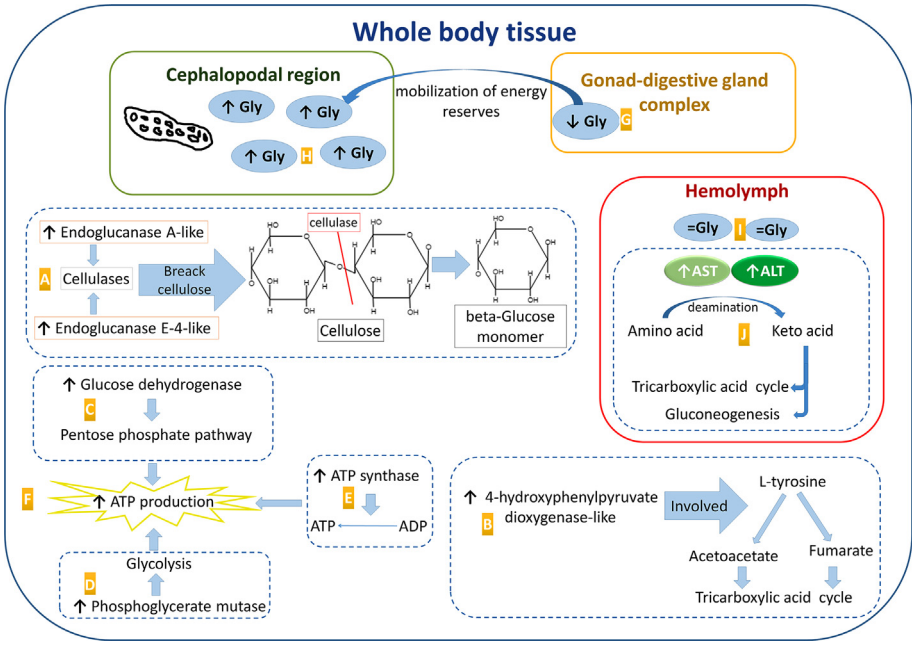

Fig. 7. Energy metabolism-associated changes in *Biomphalaria glabrata* 24 h post exposure to *Schistosoma mansoni*. (A) Endoglucanase A-like and endoglucanase E-4-like were found to be up-regulated. Both cellulases break down cellulose into monosaccharides such as β-glucose. (B) Up-regulation of 4-hydroxyphenylpyruvate dioxygenase-like, one of the enzymes involved in the conversion of L-tyrosine into acetoacetate and fumarate, which are then forward to the tricarboxylic acid cycle. (C) Up-regulation of glucose dehydrogenase (FAD, quinone)-like, an oxidoreductase which participates in the pentose phosphate pathway. (D) Up-regulation of phosphoglycerate mutase, an enzyme involved in glycolysis. (E) Up-regulation of ATP synthase subunit beta, mitochondrial protein, an enzyme involved in the conversion of ADP into ATP. (F) Apparent increase in ATP production indicating higher energetic needs. (G) Decrease in glycogen (Gly) content in the gonad-digestive complex. (H) Increase in glycogen concentration in the cephalopodal region where the parasite is present. (I) Hemolymph glycogen content without significant changes. (J) Aspartate and alanine aminotransferase activity increased, indicating an increased deamination of amino acids, which are then forwarded towards the tricarboxylic acid cycle and gluconeogenesis.

Down-regulation of this protein in exposed snails happens, most likely, due to these anti-adhesive properties, since they would interfere with the mollusk's attempt to encapsulate the parasite (Fig. 6I).

It is interesting to notice that among down-regulated proteins in exposed snails, we found two immune response proteins. Biomphalysin (Fig. 6K), a pore-forming aerolysin known for having cytolytic activity against sporocysts (Galinier et al., 2013), and Cathepsin L1-like protein (Fig. 6J). Cathepsin L1-like function in *B. glabrata* is not fully understood, however in mammals cathepsins are involved in processing functions of mammalian Antigen

Presenting Cells, while in *Drosophila* cathepsin L is present in small granules in hemocytes and is speculated to be involved in phagocytosis (Lefebvre et al., 2008). It would be expected that both proteins would be over-expressed in exposed snails, however we found them to be down-regulated. In work by Myers et al. (2008), exposed susceptible snails had lower expression of the cathepsin B transcript compared with resistant snails, whilst Arican-Goktas et al. (2014) have shown that *S. mansoni* was able to reposition activated genes, up regulating HSP-70, while in resistant snails such repositioning did not occur. It is possible that a similar process occurs, where the parasite down-regulates biomphalysin and cathepsin to successfully infect the intermediate host.

Although there is a lack of information regarding the specific function of proteins in *B. glabrata*, it is possible to find a parallel by looking at homologous proteins in other organisms. Overall, we found an activity increase in several energy-related pathways, showing a higher energy requirement by the snail after exposure to the parasite. Also, in this work, not only did we find several proteins with immune potential that were up regulated 24 h pe, but we also found down-regulated proteins such as biomphalysin, suggesting that the parasite might somehow regulate their expression. Comprehending these changes is of great importance in gaining an understanding of the host-parasite relationship.

Acknowledgments

This study was financed by Fundação de Amparo à Pesquisa do Estado de São Paulo, Brasil (FAPESP, Grant # 2016/07137-0, 2017/07364-9, and 2009/54040-8), and in part by the Coordenação de Aperfeiçoamento de Pessoal de Nível Superior, Brasil (CAPES), Finance Code – 001 as a fellowship to T.M.F.M. and Finance Code 1742613 as a fellowship to C.A.G..

Appendix A. Supplementary data

Supplementary data to this article can be found online at https://doi.org/10.1016/j.ijpara.2019.08.001.

References

Adema, C.M., Hanington, P.C., Lun, C.-M., Rosenberg, G.H., Aragon, A.D., Stout, B.A., Lennard Richard, M.L., Gross, P.S., Loker, E.S., 2010. Differential transcriptomic responses of *Biomphalaria glabrata* (Gastropoda, Mollusca) to bacteria and metazoan parasites, *Schistosoma mansoni* and *Echinostoma paraensei* (Digenea, Platyhelminthes). Mol. Immunol. 47, 849–860.

Adema, C.M., Hillier, L.W., Jones, C.S., Loker, E.S., Knight, M., Minx, P., Oliveira, G., 2017. Whole genome analysis of a schistosomiasis-transmitting freshwater snail. Nat. Commun. 8, 15451.

Arican-Goktas, H.D., Ittiprasert, W., Bridger, J.M., Knight, M., 2014. Differential spatial repositioning of activated genes in *Biomphalaria glabrata* snails infected with *Schistosoma mansoni*. PLoS Negl. Trop. Dis. 8, e3013.

Bayne, C.J., 2009. Successful parasitism of vector snail *Biomphalaria glabrata* by the human blood fluke (trematode) *Schistosoma mansoni*: a 2009 assessment. Mol. Biochem. Parasitol. 165, 8–18.

Becker, W., Schmale, H., 1975. The nitrogenous products of degradation—ammonia, urea and uric acid—in the hemolymph of the snail *Biomphalaria glabrata*. Comp. Biochem. Physiol. 51A, 407–411.

Bender, R.C., Goodall, C.P., Blouin, M.S., Bayne, C.J., 2007. Variation in expression of *Biomphalaria glabrata* SOD1: a potential controlling factor in susceptibility/resistance to *Schistosoma mansoni*. Dev. Comp. Immunol. 31, 874–878.

Bouchut, A., Coustau, C., Gourbal, B., Mitta, G., 2007. Compatibility in the *Biomphalaria glabrata*/*Echinostoma caproni* model: new candidate genes evidenced by a suppressive subtractive hybridization approach. Parasitology 134, 575–588.

Campos, Y.R., Carvalho, O.S., Goveia, C.O., Romanha, A.J., 2002. Genetic variability of the main intermediate host of the *Schistosoma mansoni* in Brazil, *Biomphalaria glabrata* (Gastropoda: Planorbidae) assessed by SSR–PCR. Acta Trop. 83, 19–27.

Cheng, T.C., Lee, F.O., 1971. Glucose levels in the mollusc *Biomphalaria glabrata* infected with *Schistosoma mansoni*. J. Invertebr. Pathol. 18, 395–399.

Chilcote, M.E., Wasson, R.D., 1958. A new micro method for the colorimetric determination of calcium in serum or urine. Clin. Chem. 4, 200–210.

Christie, J.D., Foster, W.B., Stauber, L.A., 1974. 14C Uptake by *Schistosoma mansoni* from *Biomphalaria glabrata* exposed to 14C-glucose. J. Invertebr. Pathol. 23, 297–302.

Coustau, C., Gourbal, B., Duval, D., Yoshino, T.P., Adema, C.M., Mitta, G., 2015. Advances in gastropod immunity from the study of the interaction between the snail *Biomphalaria glabrata* and its parasites: a review of research progress over the last decade. Fish Shellfish Immunol. 46, 5–16.

Cox, J., Mann, M., 2008. MaxQuant enables high peptide identification rates, individualized p.p.b.-range mass accuracies and proteome-wide protein quantification. Nat. Biotechnol. 26, 1367–1372.

de Oliveira, C.N.F., Frezza, T.F., Garcia, V.L., Figueira, G.M., Mendes, T.M.F., Allegretti, S.M., 2017. *Schistosoma mansoni: In vivo* evaluation of *Phyllanthus amarus* hexanic and ethanolic extracts. Exp. Parasitol. 183, 56–63.

de Witt, N.D., Sminia, T., 1980. The effects of the nutritional state and the external concentration of the ionic composition of the haemolymph and on calcium cells in the pulmonate freshwater snail *Lymnaea stagnalis*. Proc. Konink. Nederl. Akad. Wetenschap. 83, 213–227.

Dheilly, N.M., Duval, D., Mouahid, G., Emans, R., Allienne, J.F., Galinier, R., Genthon, C., Dubois, E., Du Pasquier, L., Adema, C.M., Grunau, C., Mitta, G., Gourbal, B., 2015. A family of variable immunoglobulin and lectin domain containing molecules in the snail *Biomphalaria glabrata*. Dev. Comp. Immunol. 48, 234–243.

Faro, M.J., Perazzini, M., Correa Ldos, R., Mello-Silva, C.C., Pinheiro, J., Mota, E.M., de Souza, S., de Andrade, Z., Junior, A.M., 2013. Biological, biochemical and histopathological features related to parasitic castration of *Biomphalaria glabrata* infected by *Schistosoma mansoni*. Exp. Parasitol. 134, 228–234.

Galinier, R., Portela, J., Mone, Y., Allienne, J.F., Henri, H., Delbecq, S., Mitta, G., Gourbal, B., Duval, D., 2013. Biomphalysin, a new beta pore-forming toxin involved in *Biomphalaria glabrata* immune defense against *Schistosoma mansoni*. PLoS Pathog. 9, e1003216.

Galinier, R., Roger, E., Mone, Y., Duval, D., Portet, A., 2017. A multistrain approach to studying the mechanisms underlying compatibility in the interaction between *Biomphalaria glabrata* and *Schistosoma mansoni*. PLoS Negl. Trop. Dis. 11, e0005398.

Giannelli, A., Cantacessi, C., Colella, V., Dantas-Torres, F., Otranto, D., 2016. Gastropod-Borne Helminths: a Look at the Snail-Parasite Interplay. Trends Parasitol. 32, 255–264.

Goodall, C.P., Bender, R.C., Brooks, J.K., Bayne, C.J., 2006. *Biomphalaria glabrata* cytosolic copper/zinc superoxide dismutase (SOD1) gene: association of SOD1 alleles with resistance/susceptibility to *Schistosoma mansoni*. Mol. Biochem. Parasitol. 147, 207–210.

Hahn, U.K., Bender, R.C., Bayne, C.J., 2001a. Involvement of nitric oxide in killing of *Schistosoma mansoni* sporocysts by hemocytes from resistant *Biomphalaria glabrata*. J. Parasitol. 87, 778–785.

Hahn, U.K., Bender, R.C., Bayne, C.J., 2001b. Killing of *Schistosoma mansoni* sporocysts by hemocytes from resistant *Biomphalaria glabrata*: role of reactive oxygen species. J. Parasitol. 87, 292–299.

Jarilla, B.R., Uda, K., Suzuki, T., Acosta, L.P., Urabe, M., Agatsuma, T., 2014. Characterization of arginine kinase from the caenogastropod *Semisulcospira libertina*, an intermediate host of *Paragonimus westermani*. J. Mollusc. Stud. 80, 444–451.

Lefebvre, C., Vandenbulcke, F., Bocquet, B., Tasiemski, A., Desmons, A., Verstraete, M., Salzet, M., Cocquerelle, C., 2008. Cathepsin L and cystatin B gene expression discriminates immune coelomic cells in the leech *Theromyzon tessulatum*. Dev. Comp. Immunol. 32, 795–807.

Lewert, R.M., Para, B.J., 1966. The physiological incorporation of carbon 14 in *Schistosoma mansoni* cercariae. J. Infect. Dis. 116, 171–182.

Lo, S., Russell, J.C., Taylor, A.W., 1970. Determination of glycogen in small tissue samples. J. Appl. Physiol. 28, 234–236.

Martins-Souza, R.L., Pereira, C.A.J., Coelho, P.M.Z., Negrão-Corrêa, D., 2003. Silica treatment increases the susceptibility of the Cabo Frio strain of *Biomphalaria tenagophila* to *Schistosoma mansoni* infection but does not alter the natural resistance of the Taim strain. Parasitol. Res. 91, 500–507.

Mello-Silva, C.C., Vilar, M.M., Vasconcellos, M.C., Pinheiro, J., Rodrigues Mde, L., 2010. Carbohydrate metabolism alterations in *Biomphalaria glabrata* infected with *Schistosoma mansoni* and exposed to *Euphorbia splendens* var. *hislopii latex*. Mem. Inst. Oswaldo Cruz 105, 492–495.

Mitta, G., Gourbal, B., Grunau, C., Knight, M., Bridger, J.M., Theron, A., 2017. The compatibility between *Biomphalaria glabrata* snails and *Schistosoma mansoni*: an increasingly complex puzzle. Adv. Parasitol. 97, 111–145.

Mone, Y., Ribou, A.C., Cosseau, C., Duval, D., Theron, A., Mitta, G., Gourbal, B., 2011. An example of molecular co-evolution: reactive oxygen species (ROS) and ROS scavenger levels in *Schistosoma mansoni*/*Biomphalaria glabrata* interactions. Int. J. Parasitol. 41, 721–730.

Mostafa, O.M., 2007. Effects of *Schistosoma mansoni* and *Schistosoma haematobium* infections on calcium content in their intermediate hosts. Parasitol. Res. 101, 963–966.

Myers, J., Ittiprasert, W., Raghavan, N., Miller, A., Knight, M., 2008. Differences in cysteine protease activity in *Schistosoma mansoni*-resistant and -susceptible *Biomphalaria glabrata* and characterization of the hepatopancreas cathepsin B Full-length cDNA. J. Parasitol. 94, 659–668.

Pereira, C.A., Martins-Souza, R.L., Coelho, P.M., Lima, W.S., Negrao-Correa, D., 2006. Effect of *Angiostrongylus vasorum* infection on *Biomphalaria tenagophila* susceptibility to *Schistosoma mansoni*. Acta Trop. 98, 224–233.

Pinheiro, J., Gomes, E.M., Chagas, G.M., 2001. Aminotransferases activity in the hemolymph of *Bradybaena similaris* (Gastropoda, Xanthonychidae) under starvation. Mem. Inst. Oswaldo Cruz 96, 1161–1164.

Sandiford, S.L., Dong, Y., Pike, A., Blumberg, B.J., Bahia, A.C., Dimopoulos, G., 2015. Cytoplasmic actin is an extracellular insect immune factor which is secreted upon immune challenge and mediates phagocytosis and direct killing of bacteria, and is a *Plasmodium Antagonist*. PLOS Pathog. 11, e1004631.

Searcy, R.L., Reardon, J.E., Foreman, J.A., 1967. A new photometric method for serum urea nitrogen determination. Am. J. Med. Technol. 33, 15–20.

Shaw, M.K., Erasmus, D.A., 1987. *Biomphalaria glabrata*: changes in calcium reserves following parasitism by larval *Schistosoma mansoni*. Parasitology 95, 267–276.

Silva, L.D., Amaral, V.C.S., Vinaud, M.C., Castro, A.M., Rezende, H.H.A., Santos, D.B., Mello-Silva, C.C., Bezerra, J.C.B., 2017. Changes in energetic metabolism of *Biomphalaria glabrata* (Mollusca, Planorbidae) in response to exogenous calcium. Braz. J. Biol. 77, 304–311.

Sminia, T., De With, N.D., Bos, J.L., Van Nieuwmegen, M.E., Witter, M.P., Wondergem, J., 1977. Structure and function of the calcium cells of the freshwater pulmonate snail *Lymnaea stagnalis*. Netherl. J. Zool. 27, 195–208.

Souza, R.M.D., Gomes, E.M., Chagas, G.M., Pinheiro, J., 2000. The influence of starvation and *Eurytrema coelomaticum* infection on the nitrogenous products of degradation in the hemolymph of *Bradybaena similaris*. Braz. Arch. Biol. Technol. 43.

Spiegel, A.M., 1987. Signal transduction by guanine nucleotide binding proteins. Mol. Cell. Endocrinol. 49, 1–16.

Tetreau, G., Pinaud, S., Portet, A., Galinier, R., Gourbal, B., Duval, D., 2017. Specific pathogen recognition by multiple innate immune sensors in an invertebrate. Front. Immunol. 8.

Tunholi-Alves, V.M., Tunholi, V.M., Garcia, J.S., Costa-Neto, S.F., Maldonado, A.J., Santos, M.A.J., Thiengo, S.C., Pinheiro, J., 2014. Changes in the calcium metabolism of *Biomphalaria glabrata* experimentally infected with *Angiostrongylus cantonensis*. J. Helminth. 88, 160–165.

Tunholi-Alves, V.M., Tunholi, V.M., Pinheiro, J., Thiengo, S.C., 2012. Effects of infection by larvae of *Angiostrongylus cantonensis* (Nematoda, Metastrongylidae) on the metabolism of the experimental intermediate host *Biomphalaria glabrata*. Exp. Parasitol. 131, 143–147.

Tyanova, S., Temu, T., Sinitcyn, P., 2016. The Perseus computational platform for comprehensive analysis of (prote)omics data. Nat. Methods 13, 731–740.

Uotila, L.M., Guenther, C., Savinko, T., Lehti, T.A., Fagerholm, S.C., 2017. Filamin A regulates neutrophil adhesion, production of reactive oxygen species, and neutrophil extracellular trap release. J. Immunol. 199, 3644–3653.

Wu, X.J., Dinguirard, N., Sabat, G., Lui, H.D., Gonzalez, L., Gehring, M., Bickham-Wright, U., Yoshino, T.P., 2017. Proteomic analysis of *Biomphalaria glabrata* plasma proteins with binding affinity to those expressed by early developing larval *Schistosoma* mansoni. PLoS Pathog. 13, e1006081.

Wu, Y., Williams, E.G., Dubuis, S., Mottis, A., Jovaisaite, V., Houten, S.M., Argmann, C. A., Faridi, P., Wolski, W., Kutalik, Z., Zamboni, N., Auwerx, J., Aebersold, R., 2014. Multilayered genetic and omics dissection of mitochondrial activity in a mouse reference population. Cell 158, 1415–1430.

Zhang, S.-M., Buddenborg, S.K., Adema, C.M., Sullivan, J.T., Loker, E.S., 2015. Altered gene expression in the schistosome-transmitting snail *Biomphalaria glabrata* following exposure to niclosamide, the active ingredient in the widely used molluscicide bayluscide. PLoS Negl. Trop. Dis. 9, e0004131.